

Supplementary Information

Oriented tube-array porous carbon anode prepared by self-blowing molding of salt templates for high-rate Potassium Storage

*Chenchen Shao, Yusheng Luo, Hongguang Fan, Yanpeng Wang, Tao Li, Qingping Li, Wei Liu**

School of Materials Science and Engineering, Ocean University of China, Qingdao 266100, People's Republic of China. Email: weiliu@ouc.edu.cn
(W. Liu)

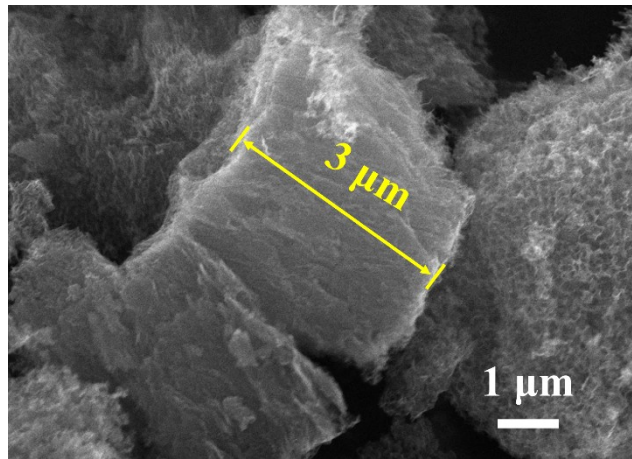


Figure S1. SEM images of TAPC samples.

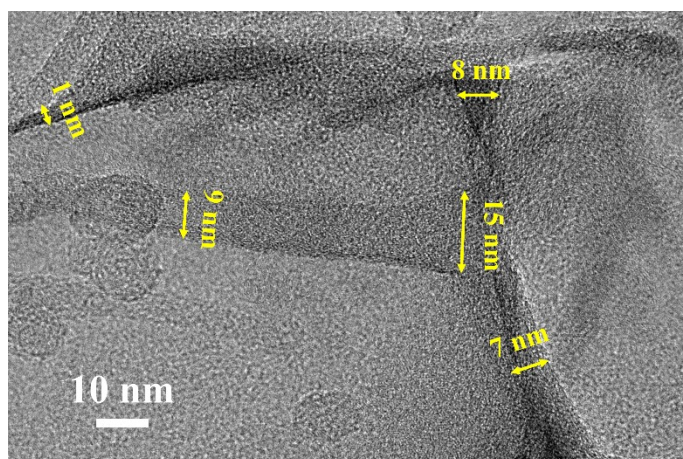


Figure S2. HRTEM images of TAPC samples.

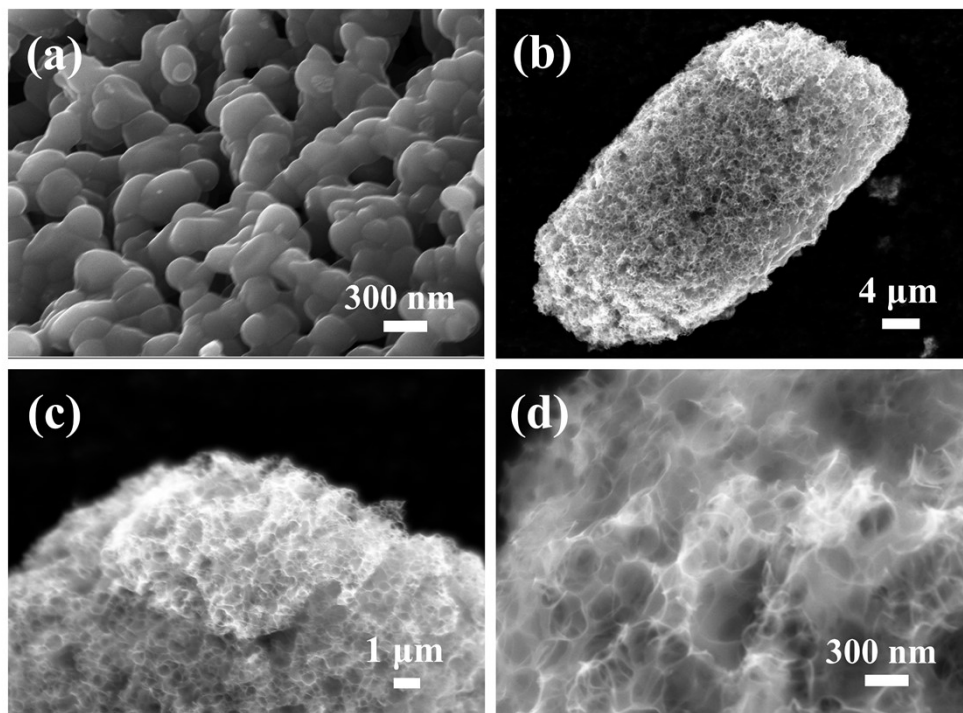


Figure S3. (a) SEM image of the Na_2CO_3 crystal skeleton obtained from the decomposition of NaHCO_3 crystal at 200°C . (b-d) SEM images of SPC samples.

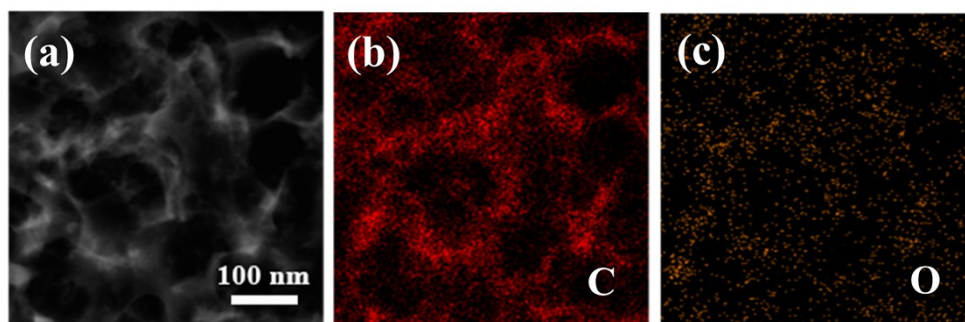


Figure S4. (a-c) EDS spectra of TAPC samples.

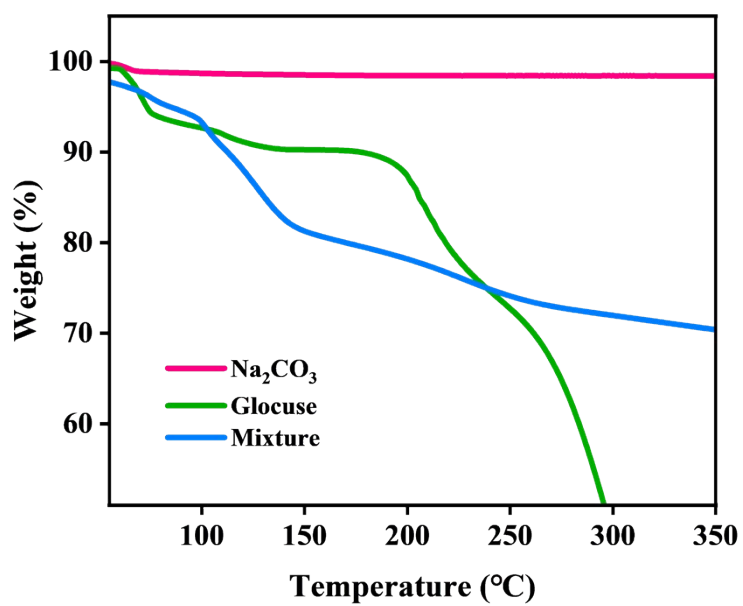


Figure S5. The TG curves of raw materials of SPC sample under nitrogen atmosphere.

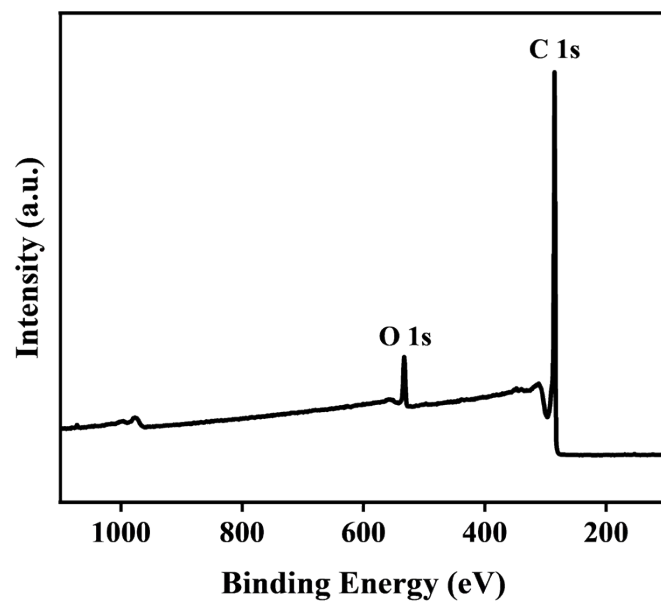


Figure S6. The XPS survey spectra of TAPC samples.

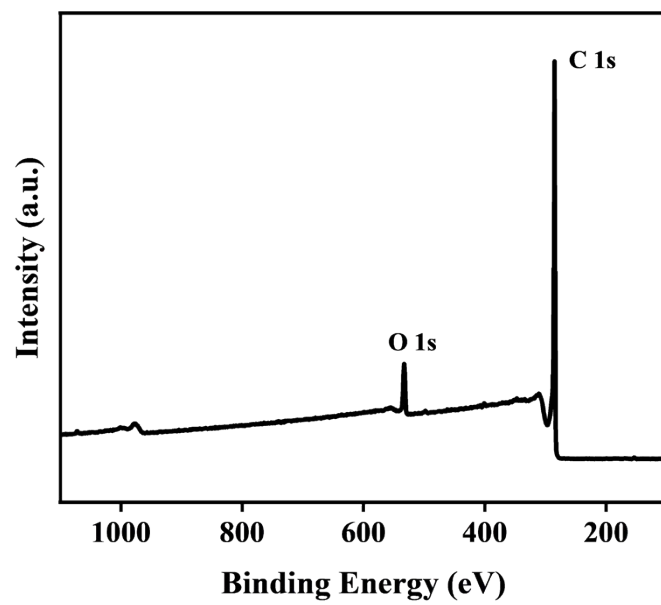


Figure S7. The XPS survey spectra of SPC samples.

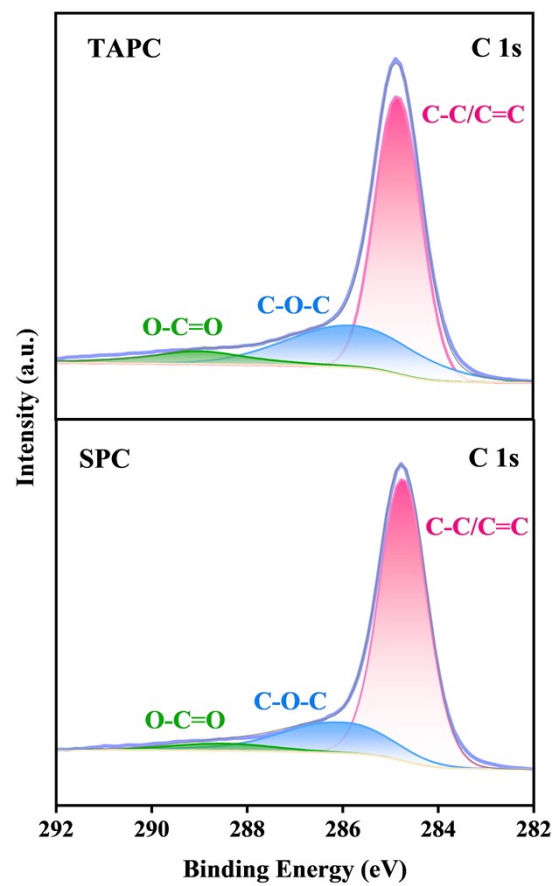


Figure S8. The high resolution XPS C 1s spectra of various samples.

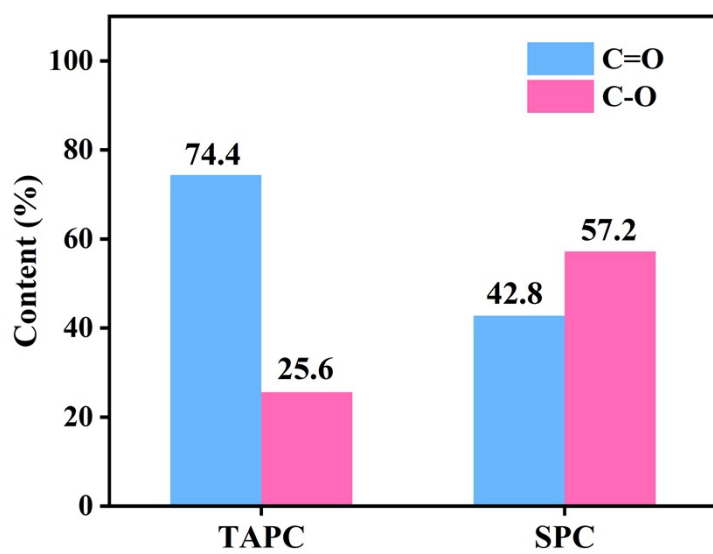


Figure S9. The content of C–O and C=O functional groups of various samples.

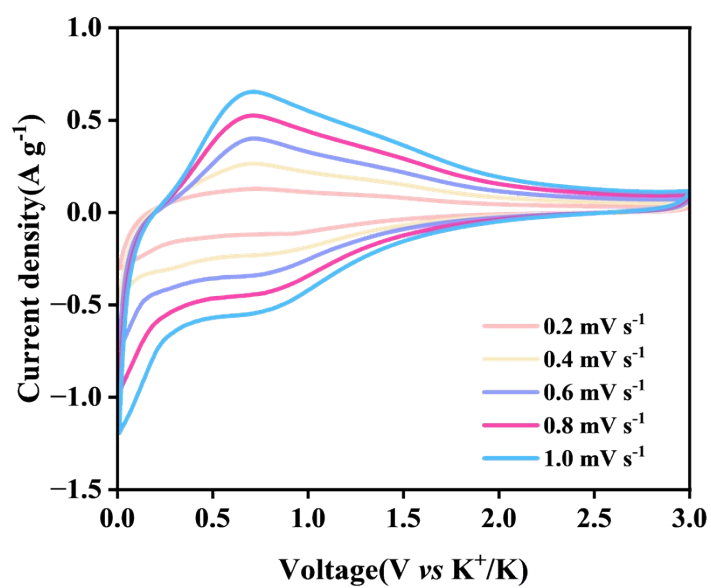


Figure S10. CV curves of SPC electrodes at different scanning rates.

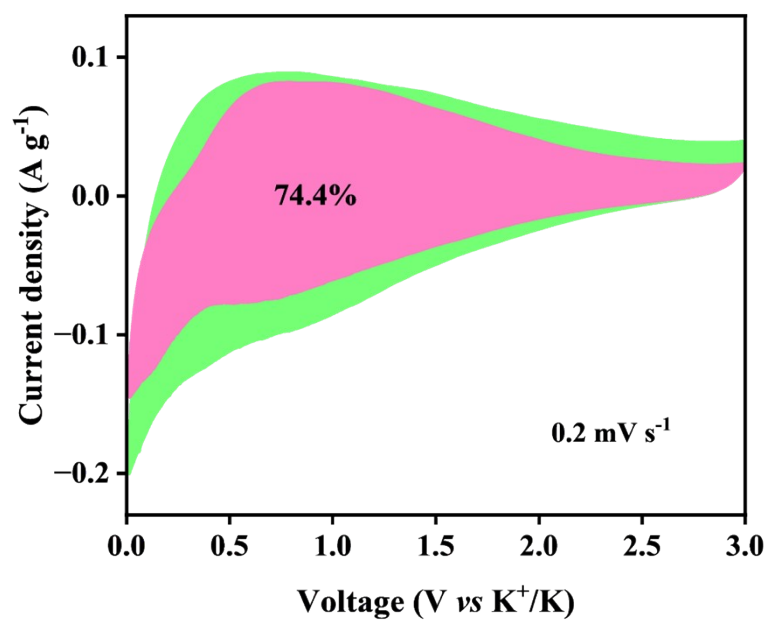


Figure S11. Contribution ratio of the capacitive-controlled and diffusion-controlled charge at 0.2 mV s^{-1} for TAPC anode.

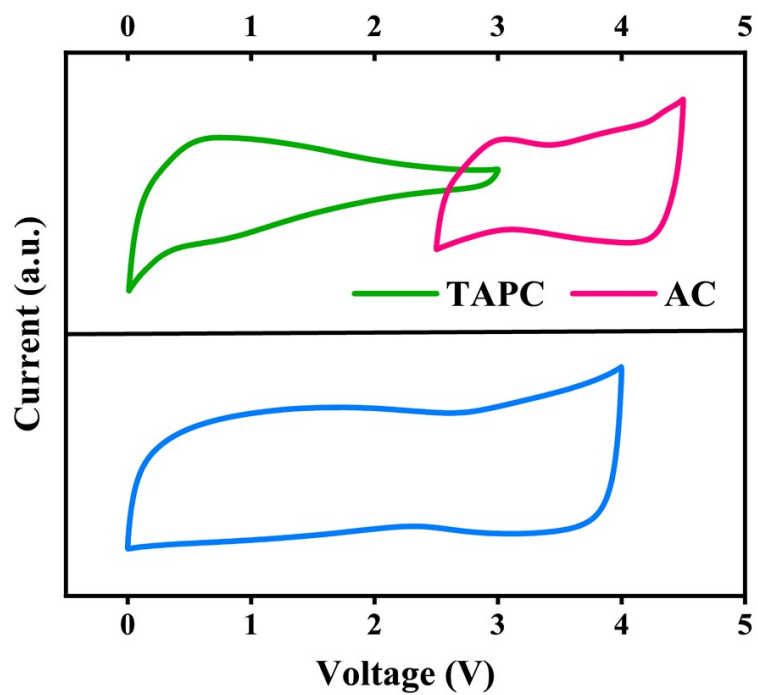


Figure S12. CV curves of TAPC and AC in K half-cell at a scan rate of 1 mV s⁻¹ (top), CV curves of TAPC//AC with a mass ratio of 1:1 (bottom).

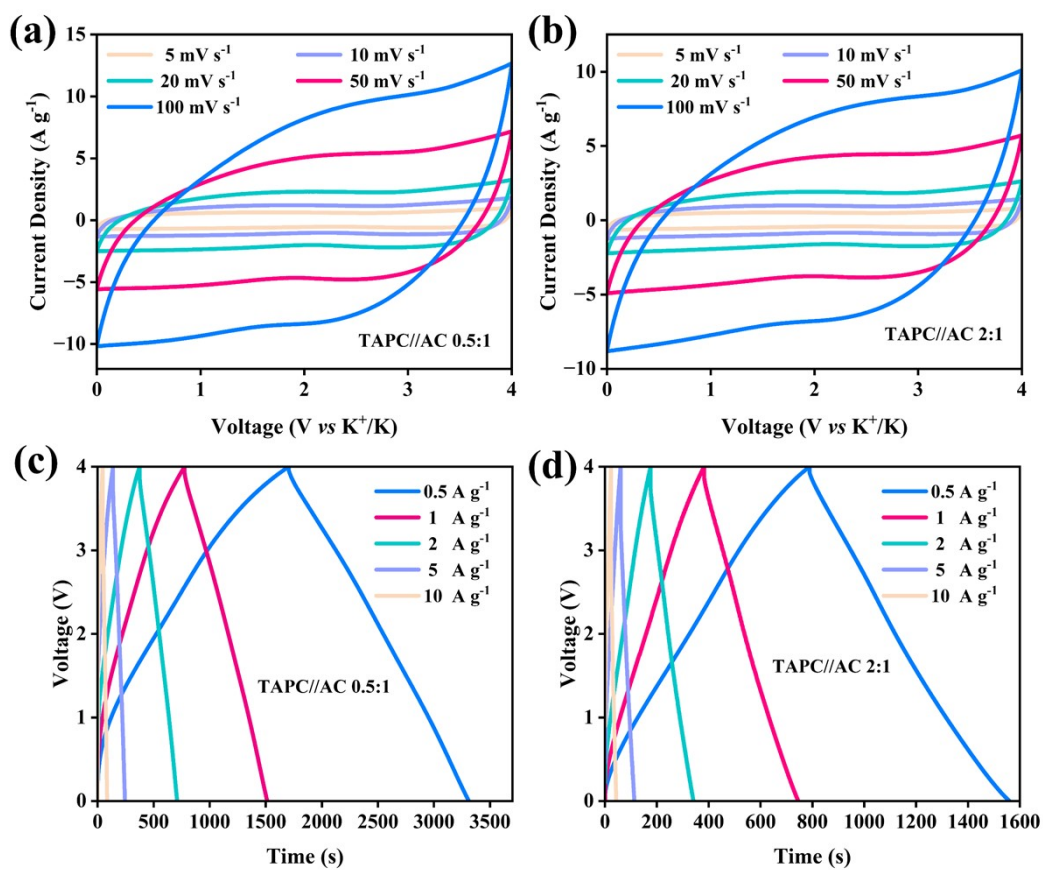


Figure S13. (a, b) CV curves at different scan rates. (c, d) Charge-discharge curves at different current densities of PIHCs with anode-to-cathode mass ratio of 0.5:1 and 2:1.



Figure S14. Ragne plots of PIHCs with various mass ratios.

Table S1. Composition of C and O element contents in various samples

| Samples | at% of total C 1s | | | at% of total O 1s | |
|---------|-------------------|-------|-------|-------------------|-------|
| | C-C//C=C | C-O-C | O-C=O | C=O | C-O |
| TAPC | 65% | 27.6% | 7.4% | 74.4% | 25.6% |
| SPC | 81% | 15.7% | 3.3% | 42.8% | 57.2% |

Table S2. Specific surface area and pore volume of various samples

| samples | S_{BET} ($\text{m}^2 \text{g}^{-1}$) | V_t ($\text{cm}^3 \text{g}^{-1}$) | Pore vol (%) | | |
|---------|---|---------------------------------------|--------------|---------|--------|
| | | | 0.3~2 nm | 2~50 nm | >50 nm |
| TAPC | 436.3 | 0.33 | 55.45 | 18.37 | 26.17 |
| SPC | 404.8 | 0.72 | 25.25 | 23.62 | 51.13 |

Table S3. Comparison of cycling performance between TAPC electrodes and other reported carbon-based anode materials for PIBs

| Sample | Cyclability | Ref. |
|---------------|--|-------------|
| This work | 244.5 mAh g ⁻¹ , 3000 cycles, 2 A g ⁻¹ | Our work |
| HG-CNTs | 191.6 mAh g ⁻¹ , 3000 cycles, 1 A g ⁻¹ | 1 |
| H-NOCBs | 178.8 mAh g ⁻¹ , 2500 cycles, 0.5 A g ⁻¹ | 2 |
| P-MgO | 178 mAh g ⁻¹ , 2000 cycles, 1 A g ⁻¹ | 3 |
| MCS | 113.9 mAh g ⁻¹ , 3600 cycles, 1 A g ⁻¹ | 4 |
| SAPC | 161.7 mAh g ⁻¹ , 2000 cycles, 1 A g ⁻¹ | 5 |
| N-C | 143 mAh g ⁻¹ , 2000 cycles, 1 A g ⁻¹ | 6 |
| SHC | 128.2 mAh g ⁻¹ , 1500 cycles, 2 A g ⁻¹ | 7 |
| SNCCs | 202.9 mAh g ⁻¹ , 1000 cycles, 2 A g ⁻¹ | 8 |
| N/P-HPCSs | 137.6 mAh g ⁻¹ , 1500 cycles, 2 A g ⁻¹ | 9 |
| HDMC | 195 mAh g ⁻¹ , 3500 cycles, 1 A g ⁻¹ | 10 |
| PGCNTs | 148.1 mAh g ⁻¹ , 950 cycles, 0.2 A g ⁻¹ | 11 |
| OLSC | 222 mAh g ⁻¹ , 1600 cycles, 1 A g ⁻¹ | 12 |
| 3D-PNC@CNTs | 143 mAh g ⁻¹ , 500 cycles, 1 A g ⁻¹ | 13 |
| CCS | 116.4 mAh g ⁻¹ , 2700 cycles, 2 A g ⁻¹ | 14 |
| HCs | 90.2 mAh g ⁻¹ , 850 cycles, 1 A g ⁻¹ | 15 |
| NPO-C-800 | 106.8 mAh g ⁻¹ , 600 cycles, 1 A g ⁻¹ | 16 |
| S-HMCNS | 197 mAh g ⁻¹ , 1400 cycles, 2 A g ⁻¹ | 17 |
| S-PC | 204.8 mAh g ⁻¹ , 3000 cycles, 1 A g ⁻¹ | 18 |

Reference

1. H. Zhang, W. Li, J. Pan, Z. Sun, B. Xiao, W. Ye, C. Ke, H. Gao, Y. Cheng, Q. Zhang and M.-S. Wang, *Journal of Energy Chemistry*, 2022, **73**, 533-541.
2. J. Li, Y. Zheng, W. Chen, W. Zhu, Y. Zhu, H. Zhao, X. Bao, L. He and L. Zhang, *Journal of Materials Chemistry A*, 2022, **10**, 17827-17837.
3. H. Tan, X. Du, R. Zhou, Z. Hou and B. Zhang, *Carbon*, 2021, **176**, 383-389.
4. J. Zheng, Y. Wu, Y. Tong, X. Liu, Y. Sun, H. Li and L. Niu, *Nano-Micro Letters*, 2021, **13**, 174.
5. J. Du, S. Gao, P. Shi, J. Fan, Q. Xu and Y. Min, *Journal of Power Sources*, 2020, **451**, 227727.
6. J. Li, Y. Li, X. Ma, K. Zhang, J. Hu, C. Yang and M. Liu, *Chemical Engineering Journal*, 2020, **384**, 123328.
7. D. Qiu, B. Zhang, T. Zhang, T. Shen, Z. Zhao and Y. Hou, *ACS Nano*, 2022, **16**, 21443-21451.
8. G. Cheng, W. Zhang, W. Wang, H. Wang, Y. Wang, J. Shi, J. Chen, S. Liu, M. Huang and D. Mitlin, *Carbon Energy*, 2022, **4**, 986-1001.
9. S. Jin, P. Liang, Y. Jiang, H. Min, M. Niu, H. Yang, R. Zhang, J. Yan, X. Shen and J. Wang, *Chemical Engineering Journal*, 2022, **435**, 134821.
10. L. Xu, Z. Gong, C. Zhang, N. Li, Z. Tang and J. Du, *Journal of Alloys and Compounds*, 2023, **934**, 167820.
11. J. Chen, G. Chen, S. Zhao, J. Feng, R. Wang, I. P. Parkin and G. He, *Small*, 2023, **19**, 2206588.
12. W. Tan, L. Wang, K. Liu, Z. Lu, F. Yang, G. Luo and Z. Xu, *Small*, 2022, **18**, 2203494.
13. P. Chen, Y. Li, X. Cheng, H. Yu, X. Yin, Y. Jiang, H. Zhang, S. Li and F. Huang, *Journal of Power Sources*, 2023, **574**, 233164.
14. Y. Chen, X. Shi, B. Lu and J. Zhou, *Advanced Energy Materials*, 2022, **12**, 2202851.
15. Z. Liu, S. Wu, Y. Song, T. Yang, Z. Ma, X. Tian and Z. Liu, *ACS Appl Mater*

Interfaces, 2022, **14**, 47674-47684.

16. H. Ou, J. Huang, Y. Zhou, J. Zhu, G. Fang, X. Cao, J. Li and S. Liang, *Chemical Engineering Journal*, 2022, **450**, 138444.

17. W. Liu, H. Zhang, W. Ye, B. Xiao, Z. Sun, Y. Cheng and M.-S. Wang, *Small*, 2023, **19**, 2300605.

18. Z. Bo, P. Chen, F. Tian, Y. Huang, Z. Zheng, J. Yan, K. Cen, H. Yang and K. Ostrikov, *Carbon*, 2023, **213**, 118261.